

An Improved Murine Premalignant Squamous Cell Model: Tobacco Smoke Exposure Augments NTCU-Induced Murine Airway Dysplasia

Lori D. Dwyer-Nield¹, Debbie G. McArthur², Meredith A. Tennis³, Daniel T. Merrick⁴, and Robert L. Keith^{2,3}



ABSTRACT

Tobacco smoke-induced squamous cell lung cancer (SCC) develops from endobronchial dysplastic lesions that progress to invasive disease. A reproducible murine model recapitulating histologic progression observed in current and former smokers will advance testing of new preventive and therapeutic strategies. Previous studies show that prolonged topical application of N-nitroso-tris-chloroethylurea (NTCU) generates a range of airway lesions in sensitive mice similar to those induced by chronic tobacco smoke exposure in humans. To improve the current NTCU model and better align it with human disease, NTCU was applied to mice twice weekly for 4–

5 weeks followed by a recovery period before cigarette smoke (CS) or ambient air (control) exposure for an additional 3–6 weeks. Despite the short time course, the addition of CS led to significantly more premalignant lesions (PML; 2.6 vs. 0.5; $P < 0.02$) and resulted in fewer alveolar macrophages (52,000 macrophages/mL BALF vs. 68,000; $P < 0.05$) compared with control mice. This improved NTCU + CS model is the first murine SCC model to incorporate tobacco smoke and is more amenable to preclinical studies because of the increased number of PML, decreased number of mice required, and reduced time needed for PML development.

Introduction

Squamous cell lung cancer (SCC) is heavily smoking related, and over 34,000 Americans will die of SCC this year (1, 2). Patients with localized non–small cell lung cancer (NSCLC) have a 61% five-year survival rate (3), indicating a critical need for improved treatment regimens, including interception in high-risk populations to prevent premalignant lesions (PML) from advancing to invasive disease. Bronchoscopy in high-risk subjects readily identifies precursor airway lesions, but a distinct minority of lesions progress to SCC. Predicting which lesions will progress, and developing strategies to target them, are major goals of current chemopreventive efforts. An improved, reproducible model of murine SCC lesion progression will advance the testing of interception strategies and help identify targetable pathways.

The mammalian respiratory epithelium is divided into tracheal, bronchial, bronchiolar, and alveolar regions (4). In humans, a pseudostratified epithelium–containing basal cells extends from the trachea through the terminal bronchioles. However, in mice this pseudostratified epithelium is restricted largely to the trachea and transitions to a simple columnar epithelium lacking basal cells in the mainstem bronchi (5). This bronchial epithelium consists of secretory club cells [club cell secretory protein (CCSP)–positive cells] and ciliated cells with motile cilia that express acetylated tubulin (ACT⁺) and lack cytokeratin (CK) 5/14 expressing basal cells (5, 6). Tracheal basal cell progenitors have been suggested as the cells of SCC origin in mice as the histopathology and gene expression of SCC lesions resembles those cells (7), but there is also evidence that forced expression of the squamous oncogene *Sox2* in Club and type II cells can also yield tumors that express SCC markers (8) but are histopathologically adenocarcinoma. In addition, Yamano and colleagues (9) identified club cells in early precancerous lesions. We previously demonstrated that N-nitroso-tris-chloroethylurea (NTCU) treatment elicited CK5⁺/K14⁺ basal stem cells in the airway of FVB/N mice before the development of dysplastic squamous lesions (10).

Currently available genetic and chemical carcinogenesis mouse SCC models are laborious, time-consuming, toxic, and typically yield low tumor numbers, making them poorly suitable for prevention studies (11, 12). Human SCC contains a large number of genetic abnormalities (13), and current genetic models often lack the mutational heterogeneity of carcinogen-induced lesions. Our group has shown that the

¹Department of Pharmaceutical Sciences, Skaggs School of Pharmacy and Pharmaceutical Sciences, University of Colorado Anschutz Medical Center, Aurora, Colorado. ²Research Division, Rocky Mountain Regional Veterans Administration Medical Center, Aurora, Colorado. ³Division of Pulmonary Sciences and Critical Care Medicine, School of Medicine, University of Colorado Anschutz Medical Center, Aurora, Colorado. ⁴Division of Pathology, School of Medicine, University of Colorado Anschutz Medical Center, Aurora, Colorado.

Corresponding Author: Robert L. Keith, Research, B151, Rocky Mountain Regional VA Medical Center, 1700 North Wheeling Street A3-350, Aurora, CO 80045. Phone: 720-857-5120; E-mail: Robert.Keith@cuanschutz.edu

Cancer Prev Res 2021;14:307–12

doi: 10.1158/1940-6207.CAPR-20-0332

©2020 American Association for Cancer Research.

topical application of NTCU leads to the appearance of basal cells and disappearance of club and ciliated cells in murine airways, subsequently generating an array of precursor lesions that progress to SCC (10). However, NTCU treatment is quite toxic, and up to 32 weeks of treatment is necessary to generate airway lesions in susceptible mouse strains, making large-scale prevention studies difficult. The mechanism by which topical application of NTCU causes lung squamous lesions is not entirely understood. Chloroethylating nitrosoureas [i.e., 1,3-bis(2-chloroethyl)-1-nitrosourea/BCNU/carmustine] are used to treat brain cancer but result in prolonged myelosuppression as well as liver and lung toxicity (14, 15). These chloroethylureas are metabolized in lung tissue (16) and alkylate DNA resulting in interstrand crosslinks (17), presumably introducing initiating mutations during DNA repair.

Herein, we report an initiation–promotion strategy, with NTCU as the initiating agent and cigarette smoke (CS) exposure for promotion, to improve the current carcinogen-induced SCC model. The introduction of CS exposure adds relevance to human disease and allows more mechanistic approaches to studying PML development. Further refinement will yield a model that can be used in multiple strains, take less time for lesion development, and allow for the application of chemopreventive agents after carcinogen exposure to more closely model former smokers.

Materials and Methods

Female A/J mice (The Jackson Laboratory) were housed in a pathogen-free facility in the Veterinary Care Unit at the Rocky Mountain Regional VA Medical Center (RMRVAMC). Studies were carried out in accordance with the recommendations in the NIH Guide for the Care and Use of Laboratory Animals and were approved by the RMRVAMC Animal Care and Use Committee. After acclimation (1–2 weeks), a 4-cm² section of skin was shaved on the dorsal region of all mice (6–8 weeks of age). Twenty-five μ L of 20 mmol/L NTCU (Toronto Research Chemicals) in acetone was applied transdermally twice weekly for 4–5 weeks on the exposed patch of skin for a total of 8 treatments. If mice lost between 15% and 20% body weight or exhibited other NTCU-induced toxicities as previously described (18), treatments were suspended until symptoms improved. After a recovery period of 1–3 weeks between NTCU and CS exposure to allow all mice to receive 8 NTCU treatments, mice were divided into 2 experimental groups (10 mice/group). One group was exposed to whole body CS at particulate levels of 35 mg/m³ and the other to ambient air in Teague Enterprises TE-10 smoking machines for 6 h/d, 5 d/wk for 3 (cohort 1) or 6 (cohort 2) weeks. Mice were weighed biweekly during NTCU exposure, daily during the first 3 weeks of CS exposure, and weekly thereafter. CS exposure was suspended in mice experiencing 15%–20% weight loss until they regained weight. Mice with advanced NTCU-induced skin lesions and/or greater than 20% weight loss were euthanized before completion of the experiment (~15% of mice/group). At the time of sacrifice, bronchoalveolar lavage (BAL) was

performed as previously described (19), and lungs were insufflated and formalin fixed for histologic analysis. Lungs from the first cohort were embedded as whole mounts to preserve architecture. In the second cohort, fixed lungs were cut into approximately 1-mm³ pieces and paraffin embedded for stereologic analysis. Differential counts using Wright stain were performed on BAL cells to compare relative alveolar macrophage numbers.

PMLs, defined as preneoplastic bronchial metaplasia and dysplasia, were detected on hematoxylin and eosin (H&E)-stained 5- μ m sections as described previously (18) and confirmed by cytokeratin 5 (CK5) IHC (Fig. 1B and C). CK5⁺ atypical epithelial was not counted as a PML unless it showed a stratified, nonciliated squamous epithelial layer with maturation in upper layers as indicated by horizontal nuclear orientation and decreased nuclear-to-cytoplasmic (N:C) ratios. Antigen retrieval of deparaffinized sections was achieved using Decloaker reagent (Biocare Medical) in an electric pressure cooker for 8 minutes, and endogenous peroxidases were quenched using Background Punisher (Biocare Medical). CK5 antibody (1:100 dilution, Biocare EP42 clone) was applied for 30 minutes at room temperature, followed by 2 washes in TBS. CK5 was visualized using the Biocare Warp Red Chromagen kit. CK5-positive dysplastic lesions were counted on 1 slide/mouse, and PML data from cohorts 1 and 2 were combined. Identification of dysplastic lesions was confirmed by a board-certified pathologist (D.T. Merrick) who was blinded to the treatment group.

Statistical analyses

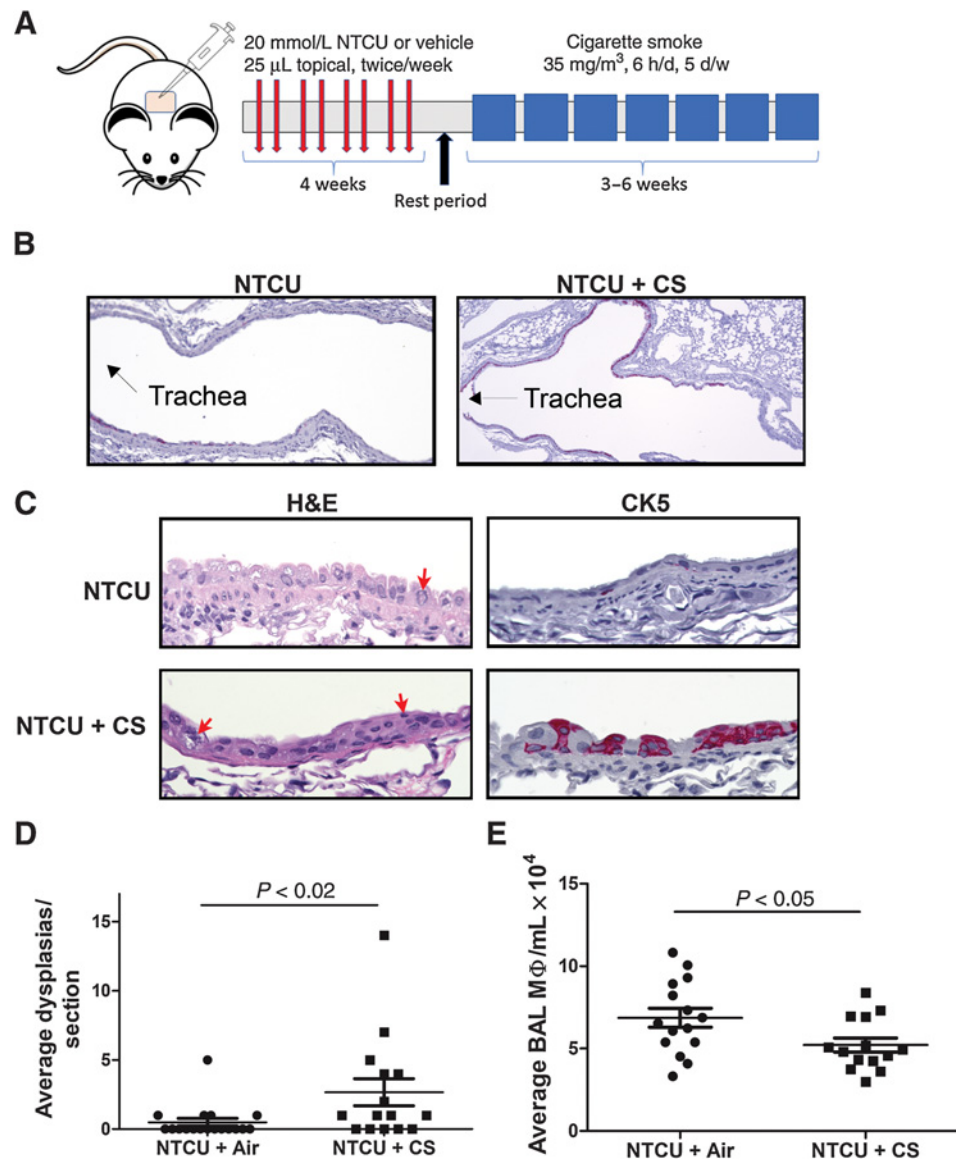
Experimental numbers were determined by power analysis using NTCU results (at 3 weeks) from Tago and colleagues (20) to detect a 30% difference in PML number with a power of 0.9, with extra mice included to account for increased toxicity with the combination of NTCU and CS. Averages were determined between groups, and groups were compared by ANOVA with Tukey *post hoc* analysis (GraphPad Prism software); A *P* value of <0.05 was considered significant.

Results

As predicted, very few dysplastic lesions developed in female A/J mice treated with NTCU alone for 9–12 weeks (Fig. 1A–C). The addition of CS to NTCU led to significant increases in PML numbers (0.5 lesions/NTCU-treated mouse vs. 2.7 in NTCU + CS mice; *P* < 0.02; Fig. 1C) and CK5 airway expression (Fig. 1A and B). Cohorts 1 and 2 exhibited similar lesion numbers, so the additional 3 weeks of smoke did not increase lesion multiplicity. Upper airways, which are normally lined with club and ciliated cells (6), exhibited CK5 staining indicative of basal cells in NTCU + CS-treated mice (Fig. 1A). Most of the CK5-positive cells localized to the mainstem bronchi adjacent to the trachea. Club and basal cell nuclei appeared dysmorphic in most of the upper airways in both NTCU and NTCU + CS-treated mice (Fig. 1B) with few apparent ciliated cells, consistent

Figure 1.

A, Schematic showing timing of NTCU and CS exposure. **B**, CK5 staining of bronchial epithelia (pink) shows the appearance of basal cells in the upper airways ($\times 4$). **C**, H&E and CK5 staining of non-dysplastic (NTCU; top) and dysplastic (NTCU/CS; bottom) airway epithelium at higher magnification ($\times 40$). Red arrows denote dysmorphic nuclei. **D**, Comparison of lesion number between NTCU and NTCU + CS-treated mice. **E**, Comparison of the BAL macrophages between NTCU and NTCU + CS mice.



with our previous results (10). No adenomas or squamous cell tumors were detected at this early time point. BAL macrophage numbers were decreased in CS exposed mice (68,000 BAL macrophages/mL in NTCU-treated mice vs. 52,000 in NTCU + CS mice; $P < 0.05$; **Fig. 1D**).

Discussion

SCC is a common, smoking-related malignancy that contains a large number of genetic mutations due to chronic tobacco smoke exposure (13). Unlike adenocarcinoma, SCC has proven difficult to model in mice. Basal cells are exceedingly rare in the normal mouse bronchial epithelium but are abundant in the trachea. Repeated NTCU skin exposure results in a gradual appearance of CK5⁺/CK14 (cytokeratin 14)⁺ basal cells and a loss of CCSP⁺ club cells

and ciliated cells in the airways, followed by the appearance of bronchial dysplasia. Although the NTCU model, first reported in 1991 (21), has been used for chemoprevention studies (22–24), adverse toxicity, lack of reproducibility, the extended time course of carcinogen exposure, and slow lesion development provide significant challenges. Tago and colleagues (20) showed rapid NTCU-induced airway dysplasia and SCC development in strain A mice, but we found A/J mice intolerant of their dosing regimen in our facility. With this extended model, the potential preventive agent is given in conjunction with the carcinogen, making it difficult to look at early tumor development and intermediate endpoints. Ideally, chemopreventive agents are administered after carcinogen exposure during early lesion development and potential progression. This models the former smoker, and multiple clinical studies have shown chemopreventive

agents to have different clinical efficacy in current and former smokers (25).

Here, we provide the initial report of an improved model that adds CS to the known SCC-inducing carcinogen NTCU in an initiation–promotion approach. Combining and shortening the customary NTCU and CS regimens ameliorated some of the toxicity, while also decreasing the time needed to develop PMLs to build a more human relevant mouse SCC model. A compressed timeline compared with the typical NTCU model (12–14 weeks vs. 32 weeks) will allow for improved testing of chemopreventive agent efficacy in PML development and progression because we have demonstrated the appearance of PML directly after NTCU + CS exposure. Clinical experience has proven that extensive preclinical testing should be conducted before preventive agents advance to clinical trials. This improved murine SCC carcinogenesis model reliably induces the appearance of basal cells in murine airways and leads to more rapid PML development. We expect that mice given an extended rest period after CS exposure will generate increased numbers of more advanced lesions that may progress to SCC, much like that seen with the Witschi CS-exposure model (26).

Many inbred mouse strains, including A/J, are exquisitely sensitive to both the toxic and carcinogenic effects of NTCU, so balancing exposure and health is an ongoing challenge. We used A/J mice for model development because these mice develop a high incidence of lung tumors in response to CS exposure (26). However, experimenting with NTCU + CS treatment in other susceptible strains (FVB and SWR) may further improve this model. SWR mice are less susceptible to the toxic effects of NTCU and can tolerate higher NTCU doses that results in a higher incidence of NTCU-induced SCC (27), whereas FVB, like A/J mice, develop CS-induced lung tumors (28). In addition, other known lung tumor-promoting agents could be combined with NTCU to improve SCC development. Of these, we have extensive experience with butylated hydroxytoluene (BHT; refs. 29, 30), which causes acute lung injury in all mouse strains and chronic inflammation in susceptible strains. We have shown that both NTCU (10) and BHT (31) injure the airway epithelium that could result in increased toxicity if not carefully administered.

The critical validation of this model will be how well it recapitulates human disease. We observed a decrease in

macrophage numbers that mirrors the macrophage decrease observed in patients with progressive dysplastic airway lesions (32) initially, indicating that this model parallels human airway injury. Our results suggest that at this early time point, inflammatory macrophages are recruited to detect and eliminate dysplastic cells, and lesions that progress have a dampened inflammatory signature resulting in less macrophage activation and recruitment. Recent studies of premalignant lung biology have demonstrated the potential importance of Wnt/ β -catenin signaling, PDL-1 activity, adaptive immune responses, and increases in proliferation and DNA repair in the progression of PML (33–36). It is critical to clarify how these mechanisms drive the change from normal to PML in the context of varying environmental and genetic insults. Insight into mechanisms of PML development will support investigation of chemoprevention in high-risk population. Further characterization of this model will continue to validate its relevance to human SCC and the updated protocol will facilitate novel studies of mechanisms of PML and opportunities for interception with chemoprevention.

Authors' Disclosures

L.D. Dwyer-Nield reports grants from Veterans Administration during the conduct of the study. R.L. Keith reports grants from Department of Veterans Affairs during the conduct of the study. No disclosures were reported by the other authors.

Authors' Contributions

L.D. Dwyer-Nield: Conceptualization, data curation, supervision, validation, methodology, writing–original draft, writing–review and editing. **D.G. McArthur:** Data curation, investigation, methodology. **M.A. Tennis:** Conceptualization, methodology, writing–review and editing. **D.T. Merrick:** Conceptualization, formal analysis, writing–review and editing. **R.L. Keith:** Conceptualization, resources, supervision, funding acquisition, writing–review and editing.

Acknowledgments

This work was supported by the Veterans Administration (Biomedical Laboratory Research and Development grant number BX000382).

The costs of publication of this article were defrayed in part by the payment of page charges. This article must therefore be hereby marked *advertisement* in accordance with 18 U.S.C. Section 1734 solely to indicate this fact.

Received June 30, 2020; revised September 25, 2020; accepted October 22, 2020; published first October 28, 2020.

References

1. Siegel RL, Miller KD, Jemal A. Cancer statistics, 2020. *CA Cancer J Clin* 2020;70:7–30.
2. Youlten DR, Cramb SM, Baade PD. The international epidemiology of lung cancer: geographical distribution and secular trends. *J Thorac Oncol* 2008;3:819–31.
3. American Cancer Society. *Cancer Facts and Figures 2020*. Atlanta: American Cancer Society; 2020.
4. Rackley CR, Stripp BR. Building and maintaining the epithelium of the lung. *J Clin Invest* 2012;122:2724–30.
5. Rock JR, Randell SH, Hogan BL. Airway basal stem cells: a perspective on their roles in epithelial homeostasis and remodeling. *Dis Model Mech* 2010;3:545–56.
6. Rock JR, Hogan BL. Epithelial progenitor cells in lung development, maintenance, repair, and disease. *Annu Rev Cell Dev Biol* 2011;27:493–512.
7. Hynds RE, Janes SM. Airway basal cell heterogeneity and lung squamous cell carcinoma. *Cancer Prev Res* 2017;10:491–3.

8. Lu Y, Futtner C, Rock JR, Xu X, Whitworth W, Hogan BL, et al. Evidence that SOX2 overexpression is oncogenic in the lung. *PLoS ONE* 2010;5:e11022.
9. Yamano S, Gi M, Tago Y, Doi K, Okada S, Hirayama Y, et al. Role of deltaNp63(pos)CD44v(pos) cells in the development of N-nitroso-tris-chloroethylurea-induced peripheral-type mouse lung squamous cell carcinomas. *Cancer Sci* 2016;107:123–32.
10. Ghosh M, Dwyer-Nield LD, Kwon JB, Barthel L, Janssen WJ, Merrick DT, et al. Tracheal dysplasia precedes bronchial dysplasia in mouse model of N-nitroso trischloroethylurea induced squamous cell lung cancer. *PLoS ONE* 2015;10:e0122823.
11. Mukhopadhyay A, Berrett KC, Kc U, Clair PM, Pop SM, Carr SR, et al. Sox2 cooperates with Lkb1 loss in a mouse model of squamous cell lung cancer. *Cell Rep* 2014;8:40–9.
12. Wang Y, Tan X, Tang Y, Zhang C, Xu J, Zhou J, et al. Dysregulated Tgfbr2/ERK-Smad4/SOX2 signaling promotes lung squamous cell carcinoma formation. *Cancer Res* 2019;79:4466–79.
13. Hammerman PS, Lawrence MS, Voet D, Jing R, Cibulskis K, Sivachenko A, et al. Comprehensive genomic characterization of squamous cell lung cancers. *Nature* 2012;489:519–25.
14. Kehrer JP, Klein-Szanto AJ. Enhanced acute lung damage in mice following administration of 1,3-bis(2-chloroethyl)-1-nitrosourea. *Cancer Res* 1985;45:5707–13.
15. Mitsudo SM, Greenwald ES, Banerji B, Koss LG. BCNU (1,3-bis-(2-chloroethyl)-1-nitrosourea) lung. Drug-induced pulmonary changes. *Cancer* 1984;54:751–5.
16. Hill DL, Kirk MC, Struck RF. Microsomal metabolism of nitrosoureas. *Cancer Res* 1975;35:296–301.
17. Ludlum DB. DNA alkylation by the haloethylnitrosoureas: nature of modifications produced and their enzymatic repair or removal. *Mutat Res* 1990;233:117–26.
18. Hudish TM, Opincariu LI, Mozer AB, Johnson MS, Cleaver TG, Malkoski SP, et al. N-nitroso-tris-chloroethylurea induces premalignant squamous dysplasia in mice. *Cancer Prev Res* 2012;5:283–9.
19. Redente EF, Orlicky DJ, Bouchard RJ, Malkinson AM. Tumor signaling to the bone marrow changes the phenotype of monocytes and pulmonary macrophages during urethane-induced primary lung tumorigenesis in A/J mice. *AmJPathol* 2007;170:693–708.
20. Tago Y, Yamano S, Wei M, Kakehashi A, Kitano M, Fujioka M, et al. Novel medium-term carcinogenesis model for lung squamous cell carcinoma induced by N-nitroso-tris-chloroethylurea in mice. *Cancer Sci* 2013;104:1560–6.
21. Rehm S, Lijinsky W, Singh G, Katyal SL. Mouse bronchiolar cell carcinogenesis. Histologic characterization and expression of Clara cell antigen in lesions induced by N-nitrosobis-(2-chloroethyl) ureas. *Am J Pathol* 1991;139:413–22.
22. Mazzilli SA, Hershberger PA, Reid ME, Bogner PN, Atwood K, Trump DL, et al. Vitamin D repletion reduces the progression of premalignant squamous lesions in the NTCU lung squamous cell carcinoma mouse model. *Cancer Prev Res* 2015;8:895–904.
23. Song JM, Qian X, Teferi F, Pan J, Wang Y, Kassie F. Dietary diindolylmethane suppresses inflammation-driven lung squamous cell carcinoma in mice. *Cancer Prev Res* 2015;8:77–85.
24. Pan J, Zhang Q, Li K, Liu Q, Wang Y, You M. Chemoprevention of lung squamous cell carcinoma by ginseng. *Cancer Prev Res* 2013;6:530–9.
25. Keith RL, Blatchford PJ, Kittelson J, Minna JD, Kelly K, Massion PP, et al. Oral iloprost improves endobronchial dysplasia in former smokers. *Cancer Prev Res* 2011;4:793–802.
26. Witschi H, Espiritu I, Dance ST, Miller MS. A mouse lung tumor model of tobacco smoke carcinogenesis. *Toxicol Sci* 2002;68:322–30.
27. Riobobos L, Gad EA, Treuting PM, Timms AE, Hershberg EA, Corulli LR, et al. The effect of mouse strain, sex, and carcinogen dose on toxicity and the development of lung dysplasia and squamous cell carcinomas in mice. *Cancer Prev Res* 2019;12:507–16.
28. Keith RL, Miller YE, Hudish TM, Girod CE, Sotto-Santiago S, Franklin WA, et al. Pulmonary prostacyclin synthase overexpression chemoprevents tobacco smoke lung carcinogenesis in mice. *Cancer Res* 2004;64:5897–904.
29. Bauer AK, Dwyer-Nield LD, Keil K, Koski K, Malkinson AM. Butylated hydroxytoluene (BHT) induction of pulmonary inflammation: a role in tumor promotion. *ExpLung Res* 2001;27:197–216.
30. Keith RL, Miller YE, Hoshikawa Y, Moore MD, Gesell TL, Gao B, et al. Manipulation of pulmonary prostacyclin synthase expression prevents murine lung cancer. *Cancer Res* 2002;62:734–40.
31. Miller AC, Dwyer LD, Auerbach CE, Miley FB, Dinsdale D, Malkinson AM. Strain-related differences in the pneumotoxic effects of chronically administered butylated hydroxytoluene on protein kinase C and calpain. *Toxicology* 1994;90:141–59.
32. Merrick DT, Edwards MG, Franklin WA, Sugita M, Keith RL, Miller YE, et al. Altered cell-cycle control, inflammation, and adhesion in high-risk persistent bronchial dysplasia. *Cancer Res* 2018;78:4971–83.
33. Aros CJ, Paul MK, Pantoja CJ, Bisht B, Meneses LK, Vijayaraj P, et al. High-throughput drug screening identifies a potent Wnt inhibitor that promotes airway basal stem cell homeostasis. *Cell Rep* 2020;30:2055–64.
34. Lee MH, Yanagawa J, Tran L, Walser TC, Bisht B, Fung E, et al. FRA1 contributes to MEK–ERK pathway-dependent PD-L1 upregulation by KRAS mutation in premalignant human bronchial epithelial cells. *Am J Transl Res* 2020;12:409–27.
35. Krysan K, Tran LM, Grimes BS, Fishbein GA, Seki A, Gardner BK, et al. The immune contexture associates with the genomic landscape in lung adenomatous premalignancy. *Cancer Res* 2019;79:5022–33.
36. Mascaux C, Angelova M, Vasaturo A, Beane J, Hijazi K, Anthoine G, et al. Immune evasion before tumour invasion in early lung squamous carcinogenesis. *Nature* 2019;571:570–5.

